



## Technical note: Optimizing the in situ cosmogenic $^{36}\text{Cl}$ extraction and measurement workflow for geologic applications

Alia J. Lesnek<sup>1,2,3</sup>, Joseph M. Licciardi<sup>1</sup>, Alan J. Hidy<sup>4</sup>, Tyler S. Anderson<sup>4</sup>

<sup>1</sup>Department of Earth Sciences, University of New Hampshire, Durham, NH 03824, USA

5 <sup>2</sup>School of Earth and Environmental Sciences, Queens College, CUNY, Flushing, NY 11367, USA

<sup>3</sup>Department of Earth and Environmental Sciences, The Graduate Center, CUNY, New York, NY 10016, USA

<sup>4</sup>Center for Accelerator Mass Spectrometry, Lawrence Livermore National Laboratory, Livermore, CA 94550, USA

*Correspondence to:* Alia J. Lesnek (alia.lesnek@qc.cuny.edu)

**Abstract.** In situ cosmogenic  $^{36}\text{Cl}$  analysis by accelerator mass spectrometry (AMS) is routinely employed to date Quaternary surfaces and assess rates of landscape evolution. However, standard laboratory preparation procedures for  $^{36}\text{Cl}$  dating require the addition of large amounts of isotopically enriched chlorine spike solution; these solutions are expensive and increasingly difficult to acquire from commercial sources. In addition, the typical workflow for  $^{36}\text{Cl}$  dating involves measuring both  $^{35}\text{Cl}/^{37}\text{Cl}$  and  $^{36}\text{Cl}/\text{Cl}$  concurrently on the high-energy (post-accelerator) end of the AMS system, but  $^{35}\text{Cl}/^{37}\text{Cl}$  determinations using this technique can be complicated by isotope fractionation and system memory during measurement. The traditional workflow also does not provide  $^{36}\text{Cl}$  extraction laboratories with the data needed to calculate native Cl concentrations in advance of  $^{36}\text{Cl}/\text{Cl}$  measurements. In light of these concerns, we present an improved workflow for extracting and measuring chlorine in geologic materials. Our initial step is to characterize  $^{35}\text{Cl}/^{37}\text{Cl}$  on up to ~1 g sample aliquots prepared in Ag(Cl, Br) matrices, which greatly reduces the amount of isotopically enriched spike solution required to measure native Cl content in each sample. To avoid potential issues with isotope fractionation through the accelerator,  $^{35}\text{Cl}/^{37}\text{Cl}$  is measured on the low-energy, pre-accelerator end of the AMS line. Then, for  $^{36}\text{Cl}/\text{Cl}$  measurements, we extract Cl as AgCl or Ag(Cl, Br) in analytical batches with a consistent total Cl load across all samples; this step is intended to minimize source memory effects during  $^{36}\text{Cl}/\text{Cl}$  measurements and allows for preparation of AMS standards that are customized to match known Cl contents in the samples. To assess the efficacy of this extraction and measurement workflow, we compare chlorine isotope ratio measurements on seven geologic samples prepared using standard procedures and the updated workflow. Measurements of  $^{35}\text{Cl}/^{37}\text{Cl}$  and  $^{36}\text{Cl}/\text{Cl}$  are consistent between the two workflows, and  $^{35}\text{Cl}/^{37}\text{Cl}$  measured using our methods have considerably higher precision than those measured following standard protocols. The chemical preparation and measurement workflow presented here (1) reduces the amount of isotopically enriched chlorine spike used per rock sample by up to 95%, (2) identifies rocks with high native Cl concentrations, which may be lower priority for  $^{36}\text{Cl}$  surface exposure dating, at an early stage of analysis, and (3) allows laboratory users to maintain control over the total chlorine content within and across analytical batches. These methods can be incorporated into existing laboratory and AMS protocols for  $^{36}\text{Cl}$  analyses and will increase the accessibility of  $^{36}\text{Cl}$  dating for geologic applications.



**Short summary:** We present an improved workflow for extracting and measuring chlorine isotopes in rocks and minerals. Experiments on seven geologic samples demonstrate that our workflow provides reliable results while offering several distinct advantages over traditional methods. Most notably, our workflow reduces the amount of isotopically enriched chlorine spike used per rock sample by up to 95%, which will allow researchers to analyze more samples using their existing laboratory supplies.

## 1 Introduction

Cosmogenic  $^{36}\text{Cl}$  is widely used within the geosciences to determine the duration of surface exposure of Quaternary features such as glacial deposits (Phillips et al., 1997; Small et al., 2016; Barth et al., 2019), lava flows (Parmelee et al., 2015; Singer et al., 2018), landslides (Ivy-Ochs et al., 2009; Zerathe et al., 2014; Pánek et al., 2018), terraces (Kozaci et al., 2007; Robertson et al., 2019), and fault scarps (Mitchell et al., 2001; Benedetti et al., 2002; Schlagenhauf et al., 2011). Over the past few decades,  $^{36}\text{Cl}$  has also emerged as the primary isotope for constraining rates of landscape evolution in carbonate settings (Stone et al., 1996; Marrero et al., 2018; Ben-Asher et al., 2021).  $^{36}\text{Cl}$  offers several advantages over other commonly used cosmogenic isotopes (e.g.,  $^{10}\text{Be}$ ) for surficial geochronology.  $^{36}\text{Cl}$  is produced by multiple reactions in a wide variety of minerals, including orthoclase, plagioclase, and calcite (Gosse and Phillips, 2001), enabling its use in dating mineral separates and whole-rock samples of nearly any lithology. The high production rate of  $^{36}\text{Cl}$  (Marrero et al., 2016) also allows for age determinations on young materials (e.g., Price et al., 2022). Additionally, accelerator mass spectrometry (AMS) measurements of chlorine (prepared as AgCl) have low detection limits and high beam currents (Finkel et al., 2013). Finally, recent advances in  $^{36}\text{Cl}$  production rate calibrations (Marrero et al., 2016) and the availability of web-based calculators (e.g., CRONUScalc, [cronus.cosmogenicnuclides.rocks/2.1/html/cl/](https://cronus.cosmogenicnuclides.rocks/2.1/html/cl/); CRONUSEarth, [stoneage.ice-d.org/math/Cl36/v3/v3\\_Cl36\\_age\\_in.html](https://stoneage.ice-d.org/math/Cl36/v3/v3_Cl36_age_in.html); CREP, <https://crep-dev.otelo.univ-lorraine.fr/#/init>) have enabled surface exposure ages or erosion rates to be determined with relative ease once total sample Cl,  $^{36}\text{Cl}$  concentration, and elemental concentrations are obtained.

In situ  $^{36}\text{Cl}$  concentrations are typically measured via AMS methods on targets prepared in an AgCl matrix (Fig. 1; Stone et al., 1996; Licciardi et al., 2008). A consistent sample mass (usually ~10-20 g of milled rock for whole-rock silicates or ~5-10 g of isolated mineral separates) is spiked with isotopically enriched Cl carrier solution such that total sample Cl (from  $^{35}\text{Cl}/^{37}\text{Cl}$ ) and  $^{36}\text{Cl}$  concentrations (from  $^{36}\text{Cl}/^{37}\text{Cl}$  or  $^{36}\text{Cl}/\text{Cl}$ ) can be determined through isotope dilution methods (Faure and Mensing, 2005). At the University of New Hampshire and the Center for AMS (CAMS) at Lawrence Livermore National Laboratory (LLNL), geologic samples have historically been spiked with ~750-1000  $\mu\text{g}$  of Cl from a  $^{37}\text{Cl}$ -enriched solution with a  $^{35}\text{Cl}/^{37}\text{Cl}$  of approximately 1, which is substantially lower than the natural  $^{35}\text{Cl}/^{37}\text{Cl}$  of 3.127. Following standard protocols (Stone et al., 1996; Licciardi et al., 2008), Cl is extracted from the samples as AgCl. After shipment to CAMS, the AgCl precipitates are packed into AgBr plugs that are pressed into open-faced stainless steel cathodes. Both  $^{35}\text{Cl}/^{37}\text{Cl}$  and  $^{36}\text{Cl}/\text{Cl}$  are then measured simultaneously on the high-energy (i.e., post-accelerator) end of the 10 MeV Tandem Van de Graaff

accelerator at CAMS, and isotope extraction laboratories receive  $^{35}\text{Cl}/^{37}\text{Cl}$  and  $^{36}\text{Cl}/\text{Cl}$  results after all measurements are completed.

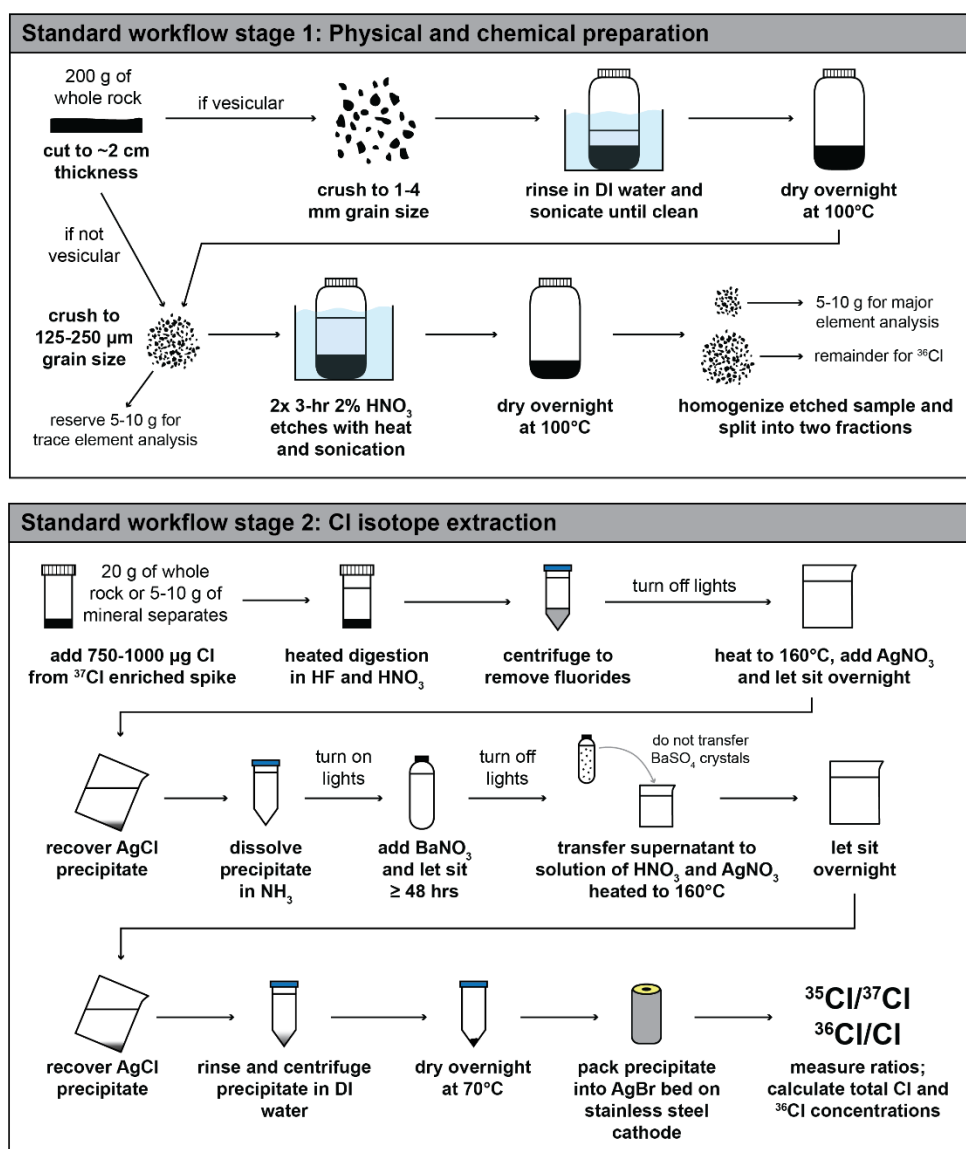


Figure 1: Schematic of the standard workflow for cosmogenic  $^{36}\text{Cl}$  analysis based on Stone et al. (1996) and Licciardi et al. (2008). Black arrows indicate the order of steps for each stage of the process.

70

While this workflow has proven useful over many years of Cl measurements at CAMS, there are several areas in which procedural and performance improvements are possible. First, few commercial sources of  $^{37}\text{Cl}$ -enriched solutions exist with negligible  $^{36}\text{Cl}$  concentrations that are acceptable as carrier for  $^{36}\text{Cl}$  sample preparation, and available source materials



are extremely expensive. Alternatively, commercial sources of  $^{35}\text{Cl}$ -enriched carrier are more readily obtained and available with negligible  $^{36}\text{Cl}$  concentrations. However, when  $^{36}\text{Cl}$ ,  $^{35}\text{Cl}$ , and  $^{37}\text{Cl}$  are measured simultaneously at the high energy end of an AMS system, it is undesirable to use carrier enriched in the more abundant isotope ( $^{35}\text{Cl}$ ). This is because it inflates the difference in intensity between  $^{35}\text{Cl}$ - and  $^{37}\text{Cl}$ - beams injected into the accelerator, leading to increased instability in maintaining terminal voltage. Considering these issues, the supply of  $^{37}\text{Cl}$ -enriched spike that is currently being used for sample preparation in extraction laboratories is limited and/or undesirable unless laboratory users have the means to invest substantial sums for new isotopically enriched chlorine solutions. Second, in the sample preparation methods outlined above, the native Cl content in each geologic sample is not known in advance of the  $^{36}\text{Cl}/\text{Cl}$  measurements, hence it is not possible to control total Cl in an analytical batch of AMS targets. Variable total Cl among samples can cause AMS memory effects after ionization of unexpectedly high Cl targets (Arnold et al., 2010; Finkel et al., 2013), and reduction of these memory effects involves longer measurement times per sample. Finally, measurements of stable Cl ratios on the high-energy, post-accelerator portion of the AMS can be affected by isotope fractionation in the terminal stripper at high ( $>40 \mu\text{A}$ )  $^{35}\text{Cl}$ - beam currents, leading to inaccurate determinations of  $^{35}\text{Cl}/^{37}\text{Cl}$  (Wilcken et al., 2013). Accurate  $^{35}\text{Cl}/^{37}\text{Cl}$  measurements are essential for determining relative contributions of different  $^{36}\text{Cl}$  production pathways to the cosmogenic  $^{36}\text{Cl}$  inventory in a sample, and for deriving the cosmogenic  $^{36}\text{Cl}$  concentration and exposure ages.

In this technical note, we present an improved laboratory and analytical workflow for measuring Cl isotope concentrations in silicate rocks via AMS. While this procedure was implemented specifically for silicates, where hydrofluoric acid (HF) is required for full digestion, it is suitable for carbonates as well by simply modifying the digestion step to exclude HF. Through a set of experiments on geologic samples, we demonstrate that the new workflow provides comparable and, in some cases, more precise results than the standard workflow. Compared to standard methods, our workflow also reduces the use of costly isotopically enriched Cl spike solution by up to 95%, which should increase the accessibility of  $^{36}\text{Cl}$  dating for geologic applications, as laboratory users can prepare more samples with their existing supplies.

## 2 Methods

Our improved cosmogenic Cl workflow involves measuring sample chloride concentrations via isotope dilution on a small ( $\sim 1 \text{ g}$ ) aliquot of rock prior to digestion of the full rock sample (Fig. 2).  $^{35}\text{Cl}/^{37}\text{Cl}$  analyses are performed on the low energy (pre-accelerator) end of an AMS with as little as  $50 \mu\text{g}$  Cl added to the target. This reduction in Cl is compensated by bulking the sample with bromine (from carrier made with commercially sourced  $\text{NH}_4\text{Br}$ ) and co-precipitating as  $\text{Ag}(\text{Cl}, \text{Br})$  to facilitate consistent sample handling and fully packed targets. Once total Cl concentrations have been determined for each sample, rock samples are prepared for  $^{36}\text{Cl}/\text{Cl}$  measurements using a modified version of standard  $^{36}\text{Cl}$  methods, with an optional addition of  $\text{NH}_4\text{Br}$  carrier at the dissolution stage for samples with low total Cl loads.  $^{36}\text{Cl}/\text{Cl}$  measurements are made on  $\text{AgCl}$  or  $\text{Ag}(\text{Cl}, \text{Br})$  targets containing a minimum of  $500 \mu\text{g}$  Cl, but ideally  $750\text{-}1000 \mu\text{g}$  Cl as  $\text{AgCl}$ .



This approach offers several advantages compared to the traditional workflow. Because Cl concentrations are  
105 determined before preparing a rock sample for  $^{36}\text{Cl}$  analysis, there is no need to add an isotopically enriched carrier solution  
to the full sample. Instead, if additional Cl is required, a carrier solution containing natural ratio Cl can be used. The natural-  
ratio Cl solution can be made with widely available and inexpensive material such as mined rock salt that is typically low in  
 $^{36}\text{Cl}$ . With this approach, each sample in an analytical  $^{36}\text{Cl}/\text{Cl}$  measurement batch is tuned to contain a similar amount of total  
chlorine, the  $^{37}\text{Cl}$ -enriched spike solution is conserved, and the presence of significant  $^{36}\text{Cl}$  in the enriched spike solution  
110 becomes a nonissue since it is used only for the stable Cl aliquots and not the target measured for  $^{36}\text{Cl}/\text{Cl}$ .

We tested this workflow on seven whole-rock geologic samples with varying silicate lithologies and a wide range of  
expected  $^{36}\text{Cl}$  inventories. For comparison, we also measured stable Cl and cosmogenic  $^{36}\text{Cl}$  on splits of the same samples  
prepared using standard procedures (Fig. 1; Stone et al., 1996; Licciardi et al., 2008). All chlorine isotope ratio measurements  
were performed at LLNL-CAMS between July 2020 and December 2023. The setup of the CAMS accelerator and operational  
115 parameters for  $^{35}\text{Cl}/^{37}\text{Cl}$  measurements are described in detail in Anderson et al. (2022).

## 2.1 Cl dilution series

To assess the accuracy of  $^{35}\text{Cl}/^{37}\text{Cl}$  measurements on the low-energy (i.e., pre-accelerator) portion of the AMS, we  
prepared a dilution series of four samples using varying amounts of  $^{37}\text{Cl}$ -enriched spike, a natural-ratio Cl carrier, and  $\text{NH}_4\text{Br}$   
carrier. For this dilution series, we used a  $^{37}\text{Cl}$ -enriched solution prepared at the University of New Hampshire (“Wildcat  
120 spike”). The Wildcat spike has a  $^{35}\text{Cl}/^{37}\text{Cl}$  of 1.001 and a Cl concentration of  $942 \pm 15 \mu\text{g g}^{-1}$  (measured via ICP-OES;  $n=4$ ;  
average  $\pm$  one standard deviation). To make the Wildcat spike, we combined  $^{37}\text{Cl}$ -enriched NaCl powder with a natural-ratio  
Cl carrier solution to achieve the desired  $^{35}\text{Cl}/^{37}\text{Cl}$  of 1.001. The isotopically enriched NaCl powder was purchased in October  
2004 from Oak Ridge National Laboratory (ORNL) and had an atomic assay of 98.21%  $^{37}\text{Cl}$  and 1.79%  $^{35}\text{Cl}$  (ORNL batch  
198501). The natural-ratio Cl carrier solution (“Weeks Island Halite carrier”) was made at the University of New Hampshire  
125 by dissolving NaCl obtained from a mine in Weeks Island, Louisiana in deionized water. The Cl concentration in the Weeks  
Island Halite carrier is  $1436 \pm 9 \mu\text{g g}^{-1}$  (measured via ICP-OES;  $n=4$ ; average  $\pm$  one standard deviation). In the dilution series,  
we adjusted the amounts of Wildcat Spike and Weeks Island Halite carrier such that total Cl in each sample was  $\sim 150 \mu\text{g}$  while  
the expected  $^{35}\text{Cl}/^{37}\text{Cl}$  values ranged from 1.001 to 2.510 (Table 1). All samples were bulked with  $\sim 4000 \mu\text{g Br}$  from a 10,000  
 $\mu\text{g g}^{-1}$   $\text{NH}_4\text{Br}$  carrier solution.

130



**Table 1: Results of  $^{35}\text{Cl}/^{37}\text{Cl}$  measurements of a dilution series to test low-energy AMS performance across a range of  $^{35}\text{Cl}/^{37}\text{Cl}$  values expected in geologic samples.**

Sample ID	Cl added from Wildcat spike ( $\mu\text{g}$ ) <sup>a</sup>	Cl added from WIH carrier ( $\mu\text{g}$ ) <sup>b</sup>	Expected $^{35}\text{Cl}/^{37}\text{Cl}$	Measured $^{35}\text{Cl}/^{37}\text{Cl}$	Measured $^{35}\text{Cl}/^{37}\text{Cl}$ uncertainty	Number of measurements	Average $^{37}\text{Cl}$ current ( $\mu\text{A}$ )	Average $^{35}\text{Cl}$ current ( $\mu\text{A}$ )
CLDSB2-1	150	0	1.001	0.997	1.66E-03	15	3.927	3.954
CLDSB2-2	94	56	1.484	1.455	2.43E-03	15	2.955	4.341
CLDSB2-3	53	98	2.016	1.997	3.33E-03	17	1.163	2.335
CLDSB2-4	25	125	2.510	2.507	4.18E-03	16	0.744	1.875

<sup>a</sup> The "Wildcat spike" has a measured  $^{35}\text{Cl}/^{37}\text{Cl}$  of 1.001 and a Cl concentration of  $942 \pm 15 \mu\text{g g}^{-1}$

<sup>b</sup> The "Weeks Island Halite" (WIH) carrier has a  $^{35}\text{Cl}/^{37}\text{Cl}$  of 3.127 (i.e., natural ratio) and a Cl concentration of  $1436 \pm 9 \mu\text{g g}^{-1}$

135 To quantify the magnitude of Cl contamination in our bromine carrier, we prepared a second dilution series using the  $^{37}\text{Cl}$ -enriched Wildcat spike and the  $\text{NH}_4\text{Br}$  carrier. We prepared four samples for this dilution series with Cl loads ranging from  $\sim 50$  to  $150 \mu\text{g Cl}$ . All samples received  $\sim 0.4 \text{ g}$  of  $10,000 \mu\text{g g}^{-1} \text{NH}_4\text{Br}$  solution ( $\sim 4000 \mu\text{g Br}$ ; Table 2). For both dilution series, after the carrier additions, the solutions were acidified in 8 mL of 2M  $\text{HNO}_3$ . To precipitate  $\text{Ag}(\text{Cl}, \text{Br})$ ,  $\sim 1 \text{ mL}$  of 5%  $\text{AgNO}_3$  was added to each solution under low light conditions and left to precipitate for at least 12 hours. The precipitates were  
140 then rinsed, dried, and packed into acid-cleaned stainless steel cathodes for  $^{35}\text{Cl}/^{37}\text{Cl}$  measurement at CAMS.

**Table 2:  $^{35}\text{Cl}/^{37}\text{Cl}$  measurements of a dilution series to test Cl contamination in the commercial  $\text{NH}_4\text{Br}$  source used in preparation of geologic test samples.**

Sample ID	Cl added from spike ( $\mu\text{g}$ ) <sup>a</sup>	Br added from carrier ( $\mu\text{g}$ ) <sup>b</sup>	Memory-corrected $^{35}\text{Cl}/^{37}\text{Cl}$	$\text{NH}_4\text{Br}$ carrier Cl concentration ( $\mu\text{g g}^{-1}$ )
CLDSA2-1	141	4099	1.009	2.14
CLDSA2-2	134	4071	1.010	2.20
CLDSA2-3	94	4101	1.011	1.76
CLDSA2-4	71	4093	1.013	1.64
CLDSA2-5	47	4072	1.012	1.02
			mean =	$1.75 \pm 0.473$

<sup>a</sup> Samples were spiked with "Wildcat Spike", which has a measured  $^{35}\text{Cl}/^{37}\text{Cl}$  of 1.001 and a Cl concentration of  $942 \pm 15 \mu\text{g g}^{-1}$ .

<sup>b</sup> The carrier solution has a concentration of  $\sim 10,000 \mu\text{g g}^{-1} \text{NH}_4\text{Br}$ .

## 145 2.2 Preparation of test samples

We prepared a set of seven geologic samples for  $^{35}\text{Cl}/^{37}\text{Cl}$  and  $^{36}\text{Cl}$  analyses (Fig. 2). Four samples (19SEAK-01, -02, -12, and -13) were collected in 2019 from two locations in coastal Southeast Alaska. 19SEAK-01 and 19SEAK-02 were sampled from erratic boulders of olivine basalt on Suemez Island (Eberlein et al., 1983) that were deposited by the Cordilleran Ice Sheet during the last deglaciation (Walcott et al., 2022). Samples 19SEAK-12 and 19SEAK-13 were obtained from the  
150 surface of a vesicular plagioclase basalt flow that was emplaced in the eastern Mount Edgecumbe Volcanic Field sometime



during the late Pleistocene (Riehle et al., 1989). Three rhyolite samples (YGT18-31, -32, and -33) were collected in 2018 from the Yellowstone Plateau. These samples were taken from the top surfaces of erratic boulders deposited during the most recent deglaciation of the Yellowstone Ice Cap (Licciardi and Pierce, 2018).

155 After initial physical and chemical preparation, we split each rock sample into two fractions. We prepared the “A” splits (e.g., 19SEAK-01A) using standard procedures (Fig. 1; Stone et al., 1996; Licciardi et al., 2008) where targets are prepared in an AgCl matrix and stable Cl ratios and cosmogenic  $^{36}\text{Cl}$  are measured concurrently on the post-accelerator end of the AMS. We used the “B” splits (e.g., 19SEAK-01B) to test the new workflow (Fig. 2). For these samples, we first characterized the stable Cl ratios and total sample Cl on a small aliquot removed from the full sample. Using this information, we then prepared the rock samples for  $^{36}\text{Cl}$  analysis.

## 160 2.2.1 Physical and chemical preparation: All test samples

We prepared all whole rock samples at the University of New Hampshire Cosmogenic Isotope Lab. Each rock sample had a starting mass of 200-300 g and a thickness of 2-3 cm. We cut some samples with a tabletop rock saw to achieve a uniform thickness. To remove dirt and other contaminants from vesicles, we first crushed samples 19SEAK-12 and 19SEAK-13 to a 1-4 mm grain size. We rinsed these two crushed samples in deionized water and sonicated them in 10-minute intervals until 165 no further material could be removed. After the initial crushing and rinsing, we dried the 1-4 mm fractions overnight at 100 °C, and then crushed all seven samples to a 125-250  $\mu\text{m}$  grain size. At this stage, we reserved 5-10 g of the 125-250  $\mu\text{m}$  size fraction for trace element analysis, which is necessary to characterize the neutron moderating properties of the rock for  $^{36}\text{Cl}$  exposure age calculations. From the remainder of the 125-250  $\mu\text{m}$  size fraction, we rinsed ~50 g in deionized water. We leached the samples in a 2%  $\text{HNO}_3$  solution for three hours in heated ultrasonic tanks, rinsed the material in deionized water, and 170 repeated the leaching for a total of two 2%  $\text{HNO}_3$  leaches. After the leached samples were dried overnight at 100°C, we divided the material into two fractions to compare results from standard preparation methods (“A” splits; Fig. 1) and the new workflow (“B” splits; Fig. 2). In the next sections, we describe the procedures used for the new workflow in detail.

## 2.2.2 Characterization of stable Cl ratios: New workflow

The goal of this step is to characterize stable chlorine ratios ( $^{35}\text{Cl}/^{37}\text{Cl}$ ) of geologic samples prior to  $^{36}\text{Cl}$  chemistry on 175 the full rock sample. For the test samples, we carried out this process on a ~1 g aliquot that was removed from the rock sample before beginning the  $^{36}\text{Cl}$  extraction (Table 3). After the two 2%  $\text{HNO}_3$  etches and subsequent drying at 100 °C, we divided the sample into three fractions using a small spoon (Fig. 2). The first fraction was the ~1 g aliquot for stable Cl analysis. The second fraction consisted of ~5-10 g for major element analysis, which is necessary to characterize  $^{36}\text{Cl}$  production rates for exposure dating purposes. We reserved the remaining material for  $^{36}\text{Cl}$  measurements. To assess the effect of sample 180 homogenization prior to splitting on measured total Cl concentration, we also prepared aliquots of four samples (19SEAK-01, -02, -12, and YGT18-31) using a micro riffle splitter (rather than a spoon) to separate the subsamples from the full rock.

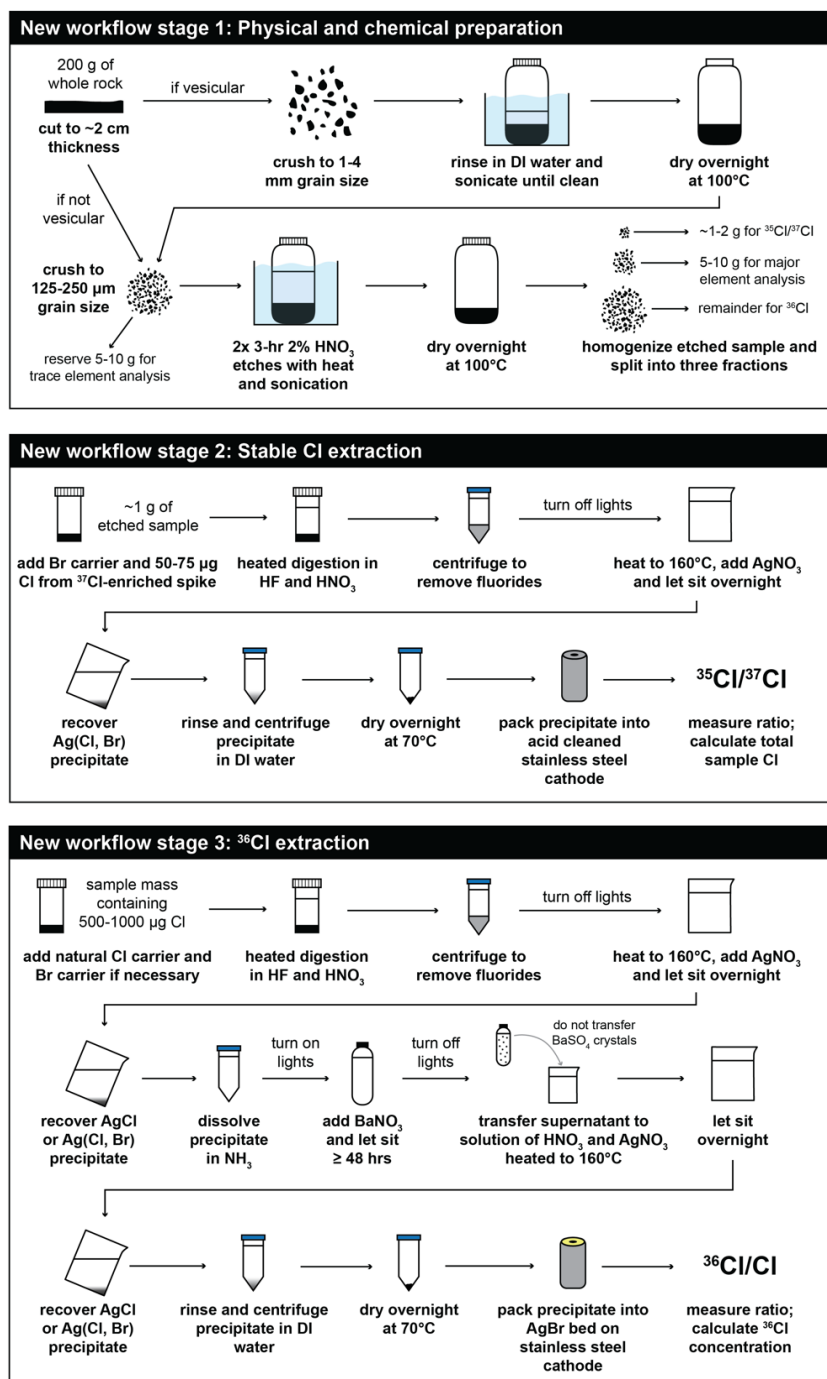


Figure 2: Schematic of the new workflow for cosmogenic <sup>36</sup>Cl analysis presented here. Black arrows indicate the order of steps for each stage of the process.





We measured  $^{35}\text{Cl}/^{37}\text{Cl}$  on Ag(Cl, Br) targets prepared using the ~1 g aliquots of etched rock sample. To prepare the Ag(Cl, Br) targets, we spiked the aliquots with a small amount of LLNL Spike A (Cl concentration =  $1284 \pm 4 \mu\text{g g}^{-1}$ ,  $^{35}\text{Cl}/^{37}\text{Cl} = 0.934$ ), totalling ~75  $\mu\text{g}$  of Cl. We then added ~4000  $\mu\text{g}$  of bromine to each sample using our  $\text{NH}_4\text{Br}$  carrier solution. To promote dissolution, we heated the spiked aliquots to 70 °C for 24-48 hours in a solution containing 4 mL of concentrated puriss HF and 6 mL 2M  $\text{HNO}_3$  per gram of sample. After dissolution, we removed fluoride compounds by centrifuging. To precipitate Ag(Cl, Br), we added ~1 mL of 5%  $\text{AgNO}_3$  to the supernatants in low light conditions and left the solutions to sit in a darkened room. After at least 12 hours, we recovered the Ag(Cl, Br) precipitates and transferred them and a small amount of supernatant to centrifuge tubes. We vortexed the solutions, then let the precipitates settle for at least 5 minutes while periodically tapping the bases of the tubes on a table. Then, we centrifuged the tubes to collect the precipitates. All samples underwent two cycles of vortexing, settling, and centrifuging while still in acidic solutions, which facilitated scavenging and flocculation of colloidal Ag(Cl, Br). We then discarded the acidic supernatants and rinsed the precipitates with deionized water. With the Ag(Cl, Br) precipitates now in water, we repeated the vortexing, tapping, and centrifuging steps twice to fully rinse the material and remove residual acids. After discarding the water, we dried the precipitates overnight at 70 °C. Finally, we packed the Ag(Cl, Br) precipitates into nitric acid cleaned stainless steel cathodes for AMS measurement of  $^{35}\text{Cl}/^{37}\text{Cl}$  at CAMS.

We prepared aliquots for  $^{35}\text{Cl}/^{37}\text{Cl}$  measurements in two analytical batches in July 2020 and February 2021, respectively. We used  $^{35}\text{Cl}/^{37}\text{Cl}$  and batch-specific process blanks (Table 3) to calculate total sample chloride through standard isotope dilution methods (Faure and Mensing, 2005). Aliquots for the analytical batch prepared in July 2020 were not separated from the full sample using a micro riffle splitter. The total Cl concentrations for these samples were corrected using process blank CLBLK-AQ6 (measured  $^{35}\text{Cl}/^{37}\text{Cl} = 0.938 \pm 0.0102$ ). Aliquots for the batch prepared in February 2021 were separated from the full sample after homogenization with a micro riffle splitter. Total sample Cl concentrations for the February 2021 batch were corrected using process blank CLBLK-AQ8 (measured  $^{35}\text{Cl}/^{37}\text{Cl} = 0.936 \pm 0.0006$ ).

### 2.2.3 Characterization of cosmogenic $^{36}\text{Cl}$ : New workflow

We characterized cosmogenic  $^{36}\text{Cl}$  concentrations for the new workflow (“B”) splits on Ag(Cl, Br) matrices prepared from  $\leq 20$  g of  $\text{HNO}_3$ -etched rock sample. We carried out the  $^{36}\text{Cl}$  extractions in two analytical batches in August 2021 and May 2021. Because we determined the total sample chloride content prior to chemistry on the full sample, we were able to adjust the amount of rock sample and natural-ratio Weeks Island Halite carrier used for  $^{36}\text{Cl}$  analyses to ensure consistent total Cl among all targets in each analytical batch (Table 4). For higher-Cl samples (YGT18-32B and YGT18-33B), no natural-ratio Cl carrier was needed, and the optimal target amount of Cl in the Ag(Cl, Br) target (~750-1000  $\mu\text{g}$  Cl) was achieved by adjusting the amount of rock digested. For low-Cl samples, the optimal total Cl was achieved by adding an appropriate amount of natural-ratio Weeks Island Halite carrier.



**Table 3: Laboratory information for test sample  $^{35}\text{Cl}/^{37}\text{Cl}$  measurements and total Cl concentration determinations.**

Sample ID	Sample mass (g)	Cl added from spike <sup>a</sup> (µg)	Memory-corrected $^{35}\text{Cl}/^{37}\text{Cl}$	$^{35}\text{Cl}/^{37}\text{Cl}$ uncertainty	Blank-corrected total sample Cl (µg)	Sample Cl concentration (µg g <sup>-1</sup> )
<b>Alaskan basalt samples</b>						
19SEAK-01A <sup>b</sup>	20.1881	773	1.272	0.0132	292.1	14.5 ± 1.4
19SEAK-01B-1 <sup>c</sup>	1.2063	79	1.133	0.0056	16.2	13.5 ± 0.1
19SEAK-01B-2 <sup>d</sup>	1.1484	75	1.110	0.0004	13.7	11.9 ± 0.1
19SEAK-02A <sup>b</sup>	20.1015	774	1.104	0.0214	132.4	6.6 ± 1.6
19SEAK-02B-1 <sup>c</sup>	1.2054	79	1.026	0.0136	6.9	5.7 ± 1.4
19SEAK-02B-2 <sup>d</sup>	1.0383	76	1.014	0.0004	5.9	5.7 ± 0.1
19SEAK-12A <sup>b</sup>	20.0392	770	1.588	0.0265	683.0	34.1 ± 2.7
19SEAK-12B-1 <sup>c</sup>	1.2252	79	1.347	0.0058	38.0	31.0 ± 1.0
19SEAK-12B-2 <sup>d</sup>	1.0184	80	1.317	0.0005	35.5	34.8 ± 0.1
19SEAK-13A <sup>b</sup>	20.0511	775	1.579	0.0095	673.9	33.6 ± 1.4
19SEAK-13B-1 <sup>c</sup>	1.2150	79	1.377	0.0059	41.6	34.3 ± 1.0
<b>Yellowstone rhyolite samples</b>						
YGT18-31A <sup>b</sup>	20.0445	774	1.672	0.0095	821.7	41.0 ± 1.5
YGT18-31B-1 <sup>c</sup>	1.2062	79	1.439	0.0062	49.2	40.8 ± 1.1
YGT18-31B-2 <sup>d</sup>	0.9412	80	1.362	0.0005	40.4	43.0 ± 0.1
YGT18-32A <sup>b</sup>	20.0639	769	1.858	0.0101	1173.7	58.5 ± 1.8
YGT18-32B-1 <sup>c</sup>	1.2209	79	1.578	0.0068	68.4	56.0 ± 1.3
YGT18-33A <sup>b</sup>	20.0619	770	1.804	0.0095	1060.1	52.8 ± 1.7
YGT18-33B-1 <sup>c</sup>	1.2086	79	1.528	0.0066	61.1	50.5 ± 1.2
<b>Process blanks</b>						
CLBLK-23	-	774	0.940	0.0313	-	-
CLBLK-AQ6	-	78	0.938	0.0102	-	-
CLBLK-AQ8	-	77	0.936	0.0006	-	-

<sup>a</sup> All samples were spiked with "LLNL Spike A", which has a  $^{35}\text{Cl}/^{37}\text{Cl}$  of 0.934 and a Cl concentration of  $1285 \pm 4 \mu\text{g g}^{-1}$ .

<sup>b</sup> Sample prepared using standard workflow. Sample Cl concentration corrected using process blank CLBLK-23.

<sup>c</sup> Sample prepared using new workflow, without using a micro riffle splitter for homogenization.

In addition to the  $^{37}\text{Cl}$ -enriched spike, sample received  $\sim 4000 \mu\text{g Br}$  from a  $\sim 10,000 \mu\text{g g}^{-1} \text{NH}_4\text{Br}$  carrier solution. Sample Cl concentration corrected using process blank CLBLK-AQ6.

<sup>d</sup> Sample prepared using new workflow, with homogenization using a micro riffle splitter.

In addition to the  $^{37}\text{Cl}$ -enriched spike, sample received  $\sim 4000 \mu\text{g Br}$  from a  $\sim 10,000 \mu\text{g g}^{-1} \text{NH}_4\text{Br}$  carrier solution. Sample Cl concentration corrected using process blank CLBLK-AQ8.

Each analytical batch contained a single process blank with Weeks Island Halite carrier and  $\text{NH}_4\text{Br}$  carrier. To account for the variable amounts of Weeks Island Halite carrier added to samples within a batch, the process blanks received the average amount of Weeks Island Halite carrier added to the samples in the batch (Table 4). No samples or blanks received  $^{37}\text{Cl}$ -enriched spike solution for the  $^{36}\text{Cl}$  extraction. All samples and blanks received  $\text{NH}_4\text{Br}$  carrier, which served to increase the size of the final precipitate. We added enough  $\text{NH}_4\text{Br}$  carrier to each sample within an analytical batch such that the moles of  $\text{Ag}(\text{Cl}, \text{Br})$  were equivalent to the moles of  $\text{AgCl}$  when precipitating  $2000 \mu\text{g}$  of Cl. Because all samples in an analytical batch had a comparable amount of total Cl after the Weeks Island Halite carrier additions, each sample and process blank in a batch received the same amount of Br carrier.

After the Cl and Br carrier additions, we prepared the  $\text{Ag}(\text{Cl}, \text{Br})$  targets using a modified version of the procedures outlined in Stone et al. (1996) and Licciardi et al. (2008). We dissolved the sample grains in a solution containing 4 mL of concentrated puriss HF and 6 mL 2M  $\text{HNO}_3$  per gram of sample. The solutions were heated to  $\sim 70^\circ\text{C}$  and left to dissolve over



230 two to three days. After dissolution, we removed insoluble fluorides through centrifuging. We transferred the supernatants into Teflon beakers and heated them to ~160 °C before adding ~1 mL 5% AgNO<sub>3</sub> under low light conditions. Samples were left to sit in a darkened cabinet for at least 12 hours to allow Ag(Cl, Br) to precipitate. We recovered the Ag(Cl, Br) precipitates and then dissolved them in 3.6M NH<sub>3</sub>. To remove <sup>36</sup>S, an interfering isobar of <sup>36</sup>Cl, we separated Cl from S by the addition of saturated BaNO<sub>3</sub> to the sample solution. After two to three days, when BaSO<sub>4</sub> crystals had formed in all samples, we transferred  
 235 the clear supernatant to a new container. We precipitated Ag(Cl, Br) a final time by acidifying the solution with 2M HNO<sub>3</sub> and adding ~1 mL 5% AgNO<sub>3</sub>. After letting the samples sit for at least 12 hours in a darkened cabinet, we recovered the Ag(Cl, Br), rinsed the precipitate in deionized water, and dried the material at 70 °C overnight. The precipitates were then sent to CAMS where they were loaded into stainless steel targets pre-packed with AgBr and analyzed for <sup>36</sup>Cl/Cl.

240

**Table 4: Laboratory information for test sample <sup>36</sup>Cl concentration determinations.**

Sample ID	Sample mass (g)	Sample Cl concentration (µg g <sup>-1</sup> )	Cl added (µg)	Memory-corrected <sup>36</sup> Cl/Cl	Ratio uncertainty	AMS uncertainty (%)	Blank-corrected <sup>36</sup> Cl concentration (atoms g <sup>-1</sup> )	<sup>36</sup> Cl concentration uncertainty (atoms g <sup>-1</sup> )	Total measurement uncertainty (%)
<b>Alaskan basalt samples</b>									
19SEAK-01A <sup>a,c</sup>	20.188	14.5 ± 1.4	773	6.89E-14	1.95E-15	2.83%	1.08E+05	3.09E+03	2.87%
19SEAK-01B <sup>b,e</sup>	12.0014	12.7 ± 0.8 <sup>f</sup>	358	1.47E-13	3.39E-15	2.30%	1.02E+05	2.37E+03	2.33%
19SEAK-02A <sup>a,c</sup>	20.102	6.6 ± 1.6	774	9.28E-14	2.17E-15	2.34%	1.35E+05	3.18E+03	2.36%
19SEAK-02B <sup>b,e</sup>	11.5081	5.7 ± 1.3 <sup>f</sup>	435	1.74E-13	5.07E-15	2.92%	1.27E+05	3.73E+03	2.99%
19SEAK-12A <sup>a,c</sup>	20.039	34.1 ± 2.7	770	2.51E-14	1.27E-15	5.07%	4.54E+04	2.35E+03	5.17%
19SEAK-12B <sup>b,d</sup>	9.9516	32.9 ± 1.0 <sup>f</sup>	604	2.94E-14	1.63E-15	5.54%	4.27E+04	2.40E+03	5.93%
19SEAK-13A <sup>a,c</sup>	20.051	33.6 ± 1.4	775	2.60E-14	1.09E-15	4.19%	4.72E+04	2.03E+03	4.29%
19SEAK-13B <sup>b,d</sup>	16.9701	34.3 ± 1.0	308	5.81E-14	2.47E-15	4.25%	4.87E+04	2.09E+03	4.41%
<b>Yellowstone rhyolite samples</b>									
YGT18-31A <sup>a,c</sup>	20.045	41.0 ± 1.5	774	3.01E-13	5.66E-15	1.88%	6.22E+05	1.17E+04	1.88%
YGT18-31B <sup>b,e</sup>	7.9558	41.9 ± 1.0 <sup>f</sup>	157	6.13E-13	1.31E-14	2.14%	6.52E+05	1.40E+04	2.15%
YGT18-32A <sup>a,c</sup>	20.064	58.5 ± 1.8	769	2.91E-13	5.46E-15	1.88%	6.84E+05	1.29E+04	1.88%
YGT18-32B <sup>b,d</sup>	14.973	56.0 ± 1.3	0	7.33E-13	1.21E-14	1.65%	6.94E+05	1.15E+04	1.65%
YGT18-33A <sup>a,c</sup>	20.062	52.8 ± 1.7	770	2.95E-13	5.55E-15	1.88%	6.67E+05	1.25E+04	1.88%
YGT18-33B <sup>b,d</sup>	16.9742	50.5 ± 1.2	0	7.74E-13	1.96E-14	2.54%	6.61E+05	1.68E+04	2.54%
<b>Process blanks</b>									
CLBLK-23 <sup>a</sup>	-	-	774	2.59E-15	3.41E-16	13.17%	-	-	-
CLBLK-25 <sup>b</sup>	-	-	458	6.41E-15	1.95E-15	30.40%	-	-	-
CLBLK-26 <sup>b</sup>	-	-	287	2.37E-15	9.24E-16	38.99%	-	-	-

<sup>a</sup> Sample prepared using standard workflow. Sample spiked with "LLNL Spike A", which has a <sup>36</sup>Cl/<sup>37</sup>Cl of 0.93 and a Cl concentration of 1285 ± 4 µg g<sup>-1</sup>.

<sup>b</sup> Sample prepared using new workflow. Sample received "Weeks Island Halite carrier" solution, which has a <sup>36</sup>Cl/<sup>37</sup>Cl of 3.127 (i.e., natural ratio) and a Cl concentration of 1436 ± 9 µg g<sup>-1</sup>. Sample also received ~4000 µg Br from a ~10,000 µg g<sup>-1</sup> NH<sub>4</sub>Br carrier solution.

<sup>c</sup> Sample <sup>36</sup>Cl concentration corrected using process blank CLBLK-23.

<sup>d</sup> Sample <sup>36</sup>Cl concentration corrected using process blank CLBLK-25.

<sup>e</sup> Sample <sup>36</sup>Cl concentration corrected using process blank CLBLK-26.

<sup>f</sup> Sample Cl concentration used for <sup>36</sup>Cl determinations is the average of two stable Cl aliquot measurements (one sample homogenized with a riffle splitter, and one sample with no homogenization; Table 3).



### 2.3.4 Isotopic analyses and process blank corrections for $^{36}\text{Cl}$ concentrations

For both the standard method and new workflow splits,  $^{36}\text{Cl}/\text{Cl}$  measurements were conducted at LLNL-CAMS. Sample ratios were normalized to KNSTD1600, which has a nominal  $^{36}\text{Cl}/^{37}\text{Cl}$  of  $6.60 \times 10^{-12}$  and a  $^{36}\text{Cl}/\text{Cl}$  of  $1.60 \times 10^{-12}$  (Sharma et al., 1990). To account for laboratory and AMS backgrounds, we corrected all sample  $^{36}\text{Cl}$  concentrations using ratios from batch-specific process blanks. The standard method (“A”) splits were processed in a single analytical batch in November 2019 and their  $^{36}\text{Cl}$  concentrations were corrected using a batch-specific blank  $^{36}\text{Cl}/\text{Cl}$  of  $2.59 \pm 0.341 \times 10^{-15}$  (CLBLK-23; equivalent to  $7.18 \times 10^4$   $^{36}\text{Cl}$  atoms). The process blank for this batch contained 774  $\mu\text{g}$  of Cl from the  $^{37}\text{Cl}$ -enriched spike solution and no Br carrier (Table 4). The new workflow (“B”) splits were processed in two analytical batches in August 2020 and May 2021, respectively. The batch processed in August 2020 included four geologic samples and a blank (CLBLK-25) containing 458  $\mu\text{g}$  of Cl from the natural Cl ratio Weeks Island Halite carrier and  $\sim 4000$   $\mu\text{g}$  of Br from the  $\text{NH}_4\text{Br}$  carrier. Sample  $^{36}\text{Cl}$  concentrations for the August 2020 batch were corrected using a process blank  $^{36}\text{Cl}/\text{Cl}$  of  $6.41 \pm 1.95 \times 10^{-15}$  (equivalent to  $4.99 \times 10^4$   $^{36}\text{Cl}$  atoms). The batch processed in May 2021 included three geologic samples (Table 4) and a process blank (CLBLK-26) that contained 287  $\mu\text{g}$  of Cl from the natural Cl ratio Weeks Island Halite carrier and  $\sim 4000$   $\mu\text{g}$  of Br from the  $\text{NH}_4\text{Br}$  carrier. Sample  $^{36}\text{Cl}$  concentrations for the May 2021 batch were corrected using a process blank  $^{36}\text{Cl}/\text{Cl}$  of  $2.37 \pm 0.924 \times 10^{-15}$  (equivalent to  $1.16 \times 10^4$   $^{36}\text{Cl}$  atoms).

## 3 Results

### 3.1 Cl dilution series

Measurements of  $^{35}\text{Cl}/^{37}\text{Cl}$  from dilutions of the Wildcat spike and Weeks Island Halite carrier agree well with expected values over a range of 1.0 to 2.5 (Table 1; Fig. 3) with uncertainties ranging between 0.0079% and 0.032%. The close agreement between the measured and expected  $^{35}\text{Cl}/^{37}\text{Cl}$  across the range of values demonstrates that samples analyzed on the low-energy end of the AMS yield accurate and highly precise stable Cl determinations. This result represents a marked improvement over past  $^{35}\text{Cl}/^{37}\text{Cl}$  measurements on the high-energy end of the AMS, which average  $\sim 1\%$ , and demonstrates that low energy  $^{35}\text{Cl}/^{37}\text{Cl}$  measurements are a favorable alternative to traditional methods.

Measurements of  $^{35}\text{Cl}/^{37}\text{Cl}$  from dilutions of the Wildcat spike and the  $\text{NH}_4\text{Br}$  carrier ranged from 1.012 to 1.036 (Table 2). Counting uncertainties for each target ranged between 0.0045% and 0.011%. Although we observe a general trend toward increasing measured  $^{35}\text{Cl}/^{37}\text{Cl}$  in dilutions with less  $^{37}\text{Cl}$ -enriched Wildcat spike, isotope dilution calculations reveal that all dilutions contain  $< 2.5$   $\mu\text{g}$  Cl per gram of  $\text{NH}_4\text{Br}$  (mean =  $1.75 \pm 0.473$   $\mu\text{g g}^{-1}$ ); in other words, Cl contamination is negligible in our bromine carrier. Thus, the commercial  $\text{NH}_4\text{Br}$  source is suitable for the procedures presented here if samples contain at least 20  $\mu\text{g}$  of total Cl, which is well below the typical target amount for whole rock and mineral separates analyzed for cosmogenic  $^{36}\text{Cl}$  exposure dating. For samples with total Cl masses  $< 20$   $\mu\text{g}$ , alternative preparation protocols that do not

use  $\text{NH}_4\text{Br}$  carrier (e.g., Anderson et al., 2022) would be necessary. It should be noted, however, that those alternative protocols are not suitable for silicate materials that require digestion in HF during sample dissolution (*Section 4, Discussion, below*).

275

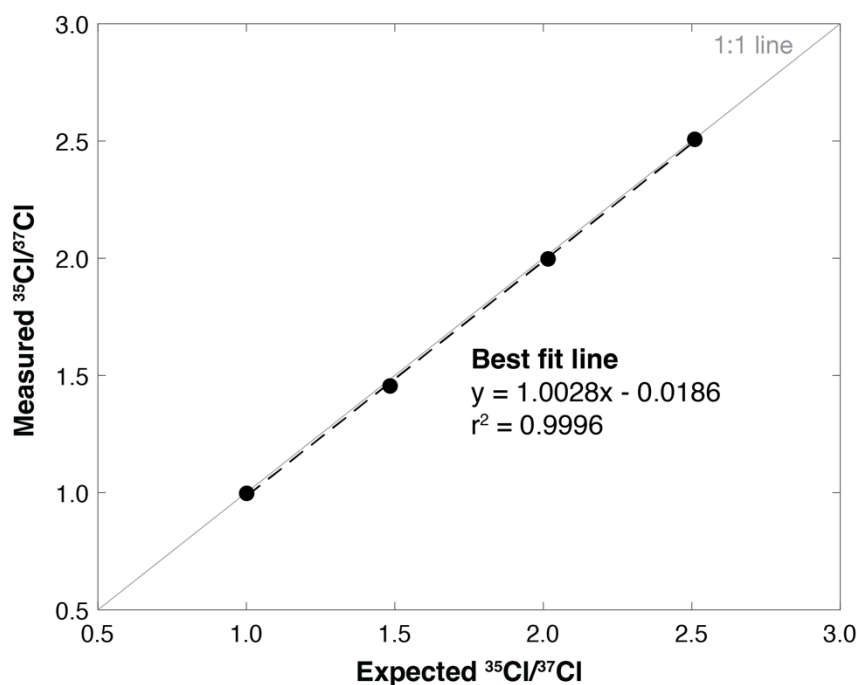
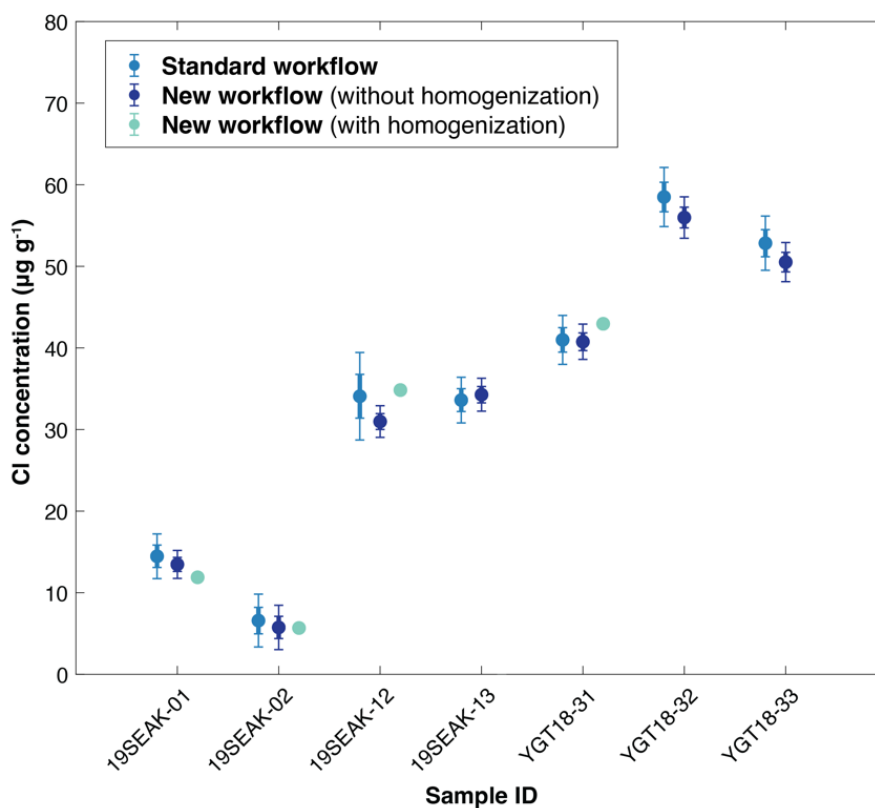


**Figure 3:** Measured vs. expected  $^{35}\text{Cl}/^{37}\text{Cl}$  for dilutions of the UNH Wildcat spike and the Weeks Island Halite carrier. Error bars on measured  $^{35}\text{Cl}/^{37}\text{Cl}$  are too small to be visible on the figure. Solid gray diagonal line shows a 1:1 relationship between expected and measured  $^{35}\text{Cl}/^{37}\text{Cl}$  and dotted black line shows the best fit line between the data points. The equation and  $r^2$  value for the best fit line are also provided.

280

### 3.2 Test samples

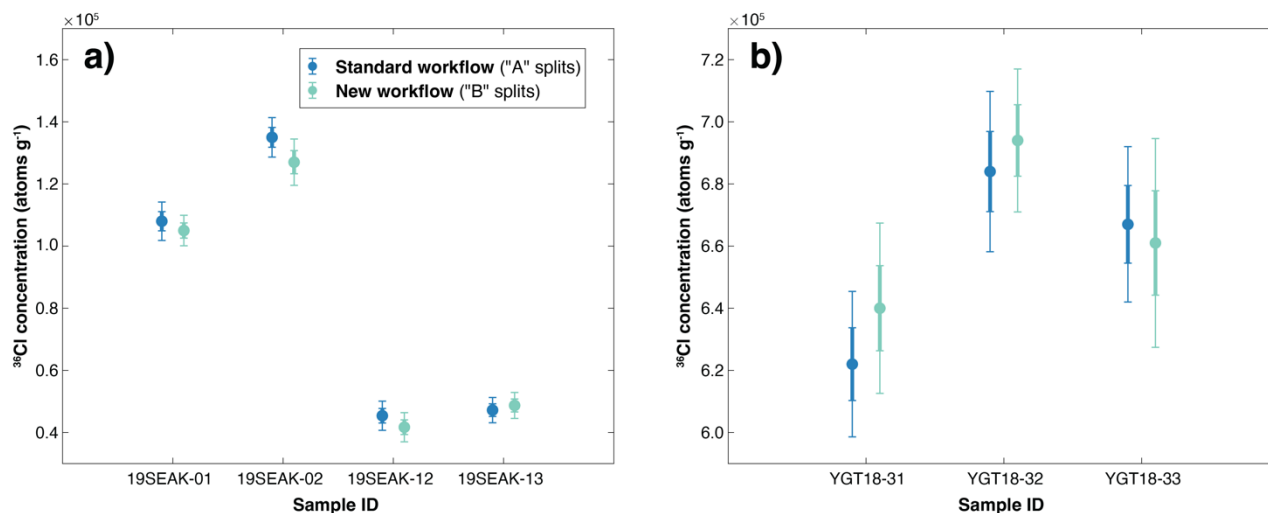
We successfully measured  $^{35}\text{Cl}/^{37}\text{Cl}$  and  $^{36}\text{Cl}/\text{Cl}$  on test samples at levels that were well above process blank values (Tables 3 and 4). For the “A” splits prepared using the standard workflow, errors on  $^{35}\text{Cl}/^{37}\text{Cl}$  measurements ranged from 0.53% to 1.93%. Measurement errors for  $^{35}\text{Cl}/^{37}\text{Cl}$  analyses on the “B” splits prepared using the new workflow presented here  
285 ranged from 0.038% to 0.43%, demonstrating that pre-accelerator measurements of stable Cl isotope ratios provide considerably higher precision than measurements on the post-accelerator end of the AMS. Blank-corrected total Cl concentrations for test samples varied from  $\sim 6 \mu\text{g g}^{-1}$  Cl for the Alaskan basalts to  $\sim 60 \mu\text{g g}^{-1}$  Cl for the Yellowstone rhyolites. (Table 3; Fig. 4). Total Cl determinations for all the “A” and “B” splits overlap within 2-sigma measurement uncertainty, regardless of whether a micro riffle splitter was used to homogenize the leached rock before dividing it into subsamples (Table  
290 3; Fig. 4).



295 **Figure 4: Comparison of total Cl concentrations ( $\mu\text{g g}^{-1}$ ) for samples measured using the standard workflow (blue dots; all samples), the new workflow with aliquots separated without homogenization (purple dots; all samples), and the new workflow with aliquots separated after homogenization with a riffle splitter (green dots; four samples only). Measurement uncertainties for each sample are shown at 1-sigma (thick vertical lines) and 2-sigma (thin vertical lines). For the four homogenized samples (green dots), uncertainties are smaller than the symbol size.**

300  $^{36}\text{Cl}$  concentrations for the standard method “A” splits ranged from  $4.54 \times 10^4$  to  $6.84 \times 10^5$  atoms  $\text{g}^{-1}$ , with total measurement uncertainties (including process blank corrections) between 1.88% and 5.17% (Table 4). For the new workflow “B” splits,  $^{36}\text{Cl}$  concentrations ranged from  $4.27 \times 10^4$  to  $6.94 \times 10^5$  atoms  $\text{g}^{-1}$ ; measurement uncertainties ranged from 1.65% to 5.93%. Uncertainties on  $^{36}\text{Cl}/\text{Cl}$  measurements are higher than on  $^{35}\text{Cl}/^{37}\text{Cl}$  measurements, which is not surprising given the much lower ratios measured for  $^{36}\text{Cl}/\text{Cl}$ .  $^{36}\text{Cl}$  concentrations for all sample pairs except 19SEAK-02 agree within 1-sigma measurement uncertainty, and all  $^{36}\text{Cl}$  concentration measurements for sample pairs agree within 2-sigma measurement uncertainty. There are no systematic variations in  $^{36}\text{Cl}$  concentration between the two preparation workflows (Fig. 5). This set of measurements demonstrates that the  $^{36}\text{Cl}$  analyses for each preparation method provide equivalent results within uncertainty.

305



310 **Figure 5: Comparison of blank-corrected  $^{36}\text{Cl}$  concentrations (atoms  $\text{g}^{-1}$ ) for the geologic test samples (a: Alaskan basalt; b: Yellowstone rhyolite) prepared using the standard workflow (“A” splits; blue dots) and the new workflow presented here (“B” splits; green dots). Measurement uncertainties for each sample are shown at 1-sigma (thick vertical lines) and 2-sigma (thin vertical lines). Although measurement uncertainties on  $^{36}\text{Cl}$  concentrations for the three YGT18 samples appear visually larger than those of the 19SEAK samples, percent uncertainties on both sets of samples are comparable (Table 4). For ease of comparison, the range of the y-axis in both panels is  $1.4 \times 10^5$  atoms  $\text{g}^{-1}$ .**

#### 4 Discussion

315 The amended cosmogenic chlorine workflow presented here offers substantial advantages over conventional protocols across all levels of analysis, spanning from laboratory preparation to AMS measurement. Measurement of  $^{35}\text{Cl}/^{37}\text{Cl}$  on the low-energy end of the AMS line with consistent and substantially smaller total Cl loads in all targets results in total uncertainties on  $^{35}\text{Cl}/^{37}\text{Cl}$  measurements of  $<1\%$ , and often  $<0.05\%$ . Rock sample chlorine concentrations can thus be determined with high precision. By characterizing  $^{35}\text{Cl}/^{37}\text{Cl}$  and total Cl prior to  $^{36}\text{Cl}$  measurement, rock samples with high Cl

320 concentrations can also be identified and screened at an earlier stage of analysis. This is important because high native Cl concentrations in rocks can result in exposure ages with comparably larger external uncertainties due to the greater uncertainty in the  $^{36}\text{Cl}$  production rate from thermal neutron capture on  $^{35}\text{Cl}$  (Marrero et al., 2016). Depending on the desired exposure age precision, these high native Cl samples may be excluded from further analysis. Furthermore, the  $^{35}\text{Cl}/^{37}\text{Cl}$  aliquot method presented here also uses only  $\sim 1$  g of etched sample to obtain total Cl concentrations. However, we note that this method can

325 be applied to substantially less material than the 1 g used here depending on a sample’s total Cl concentration, aliquot homogeneity, and the need for high precision in the Cl concentration measurement. We chose to use 1 g of etched sample to help ensure that the stable Cl aliquot was representative of the whole sample, and because we suspected some samples could have exceptionally low Cl concentrations such that 1 g would be large enough to characterize Cl at levels where the  $^{35}\text{Cl}(n,\gamma)^{36}\text{Cl}$  reaction becomes a significant contributor to total  $^{36}\text{Cl}$  production. For the method presented here, a sample size



330 equivalent to 5  $\mu\text{g}$  Cl is likely sufficient, indicating that many of our samples could have been analyzed at high precision using  
only  $\sim 0.1$  g of material. This is substantially less than the amount required for total Cl determinations by other techniques such  
as XRF, which can consume  $>10$  g of material. The small amount of material required for total Cl measurements is thus a key  
advantage when sample sizes are limited (e.g., when analyzing feldspar mineral separates). Finally, and perhaps most  
importantly for cosmogenic chlorine extraction laboratories, our workflow reduces the use of isotopically enriched chlorine  
335 spike by up to 95% compared to conventional methods, which will considerably extend the lifespan of existing laboratory  
supplies.

While our laboratory protocols offer an improvement over conventional cosmogenic chlorine preparation methods,  
there is room for further refinement. For example, Anderson et al. (2022) presented an innovative approach wherein AgCl  
targets were prepared within a niobium matrix, resulting in successful measurement of  $^{35}\text{Cl}/^{37}\text{Cl}$  on targets with Cl masses as  
340 low as 1  $\mu\text{g}$ ; they also observed a substantially reduced source memory compared to targets bulked with AgBr. However, a  
key distinction between their methodology and the one outlined here is that, unlike our silicate samples, Anderson et al.'s  
aqueous Cl samples did not require the use of HF in the dissolution process. Given niobium's solubility in HF acid, employing  
this method on silicate samples requires thorough rinsing to eliminate residual acid from AgCl precipitates before introducing  
niobium powder. HF remaining in the AgCl precipitates can also react to form fluoride compounds with an atomic mass of 35  
345 (e.g.,  $^{16}\text{O}^{19}\text{F}$ ), which can interfere with measurement of  $^{35}\text{Cl}/^{37}\text{Cl}$ . Thus, removing all HF before adding niobium to AgCl  
precipitates is critical. On the other hand, AgCl is mildly water soluble ( $\sim 2$   $\mu\text{g mL}^{-1}$ ), and extensive rinsing may reduce the  
AgCl yield. Therefore, the challenge is to rinse samples thoroughly enough to remove all traces of HF while still maintaining  
a high AgCl yield. We have attempted this process with silicate derived AgCl precipitates that contain  $\sim 50$   $\mu\text{g}$  of total Cl, but  
consistently and accurately measuring  $^{35}\text{Cl}/^{37}\text{Cl}$  on such samples has proven difficult, likely due to both yield loss during the  
350 procedure and residual HF remaining in some targets even after thorough rinsing. Refining these procedures is the focus of  
ongoing experimentation. Nevertheless, our findings unequivocally show that  $^{35}\text{Cl}/^{37}\text{Cl}$  on silicate samples can be consistently  
measured with high precision on Ag(Cl, Br) when the total chlorine mass in each target exceeds 50  $\mu\text{g}$ . Thus, while there are  
possibilities for improvement, we are confident that procedures presented herein can be deployed with little modification in  
cosmogenic chlorine laboratories and AMS facilities.

355 To implement the preparation and measurement workflow described above, we suggest three key practices. First, we  
recommend using a micro riffle splitter to separate subsamples for  $^{35}\text{Cl}/^{37}\text{Cl}$ ,  $^{36}\text{Cl}/\text{Cl}$ , and major element analyses from the full  
rock sample. The homogenization step does not appear to be strictly necessary for the two lithologies we tested here (basalt  
and rhyolite; Fig. 4). We speculate that these fine-grained igneous rocks are already quite compositionally homogenous due to  
the scarcity or lack of phenocrysts and the high percentage of groundmass, and the milled grains therefore do not separate  
360 much by composition after milling and during storage in plastic bags. However, we do encourage the use of a micro riffle  
splitter for coarse grained lithologies that may contain monomineralic grains when crushed to the 250-125  $\mu\text{m}$  size fraction we  
recommend here, as we suspect these rocks may be more susceptible to separation by composition during storage. Second, we  
stress the importance of exercising caution when cleaning stainless steel AMS cathodes prior to sample loading. Early





experiments indicated that the commercial laboratory soaps we used to clean our AMS cathodes contain chlorine that is not  
365 removed from cathode surfaces by thorough rinsing with deionized water. Therefore, we suggest that laboratory users soak  
AMS cathodes in a weak (~1%) nitric acid solution after cleaning with laboratory soap. This step is essential to eliminate  
residual natural-ratio chlorine that may contaminate the cathode surfaces and erroneously raise measured  $^{35}\text{Cl}/^{37}\text{Cl}$  on spiked  
samples. Finally, if samples are bulked with  $\text{NH}_4\text{Br}$  carrier, we recommend that laboratory users prepare “matrix blanks” of  
AgBr (with no added Cl) for measurement, which will allow for accurate ion source memory corrections for unknown samples.  
370 Consistency in target matrices across a stable Cl analysis minimizes source memory and improves ion beam stability,  
contributing to more accurate and reproducible experimental outcomes.

## 5 Conclusions

We present an improved workflow for extracting and measuring chlorine in silicate rocks. After crushing the rock  
and cleaning the mineral surfaces with dilute  $\text{HNO}_3$ , we characterize stable Cl ratios on an up to ~1 g aliquot of rock removed  
375 from the full sample.  $^{35}\text{Cl}/^{37}\text{Cl}$  is then measured on the low-energy beam line of the CAMS accelerator, allowing us to quickly  
determine total chlorine loads while minimizing source memory and substantially reducing the amount of  $^{37}\text{Cl}$ -enriched carrier  
solution used per sample. With  $^{35}\text{Cl}/^{37}\text{Cl}$  data in hand, we then extract Cl from rock samples for  $^{36}\text{Cl}/\text{Cl}$  measurements and  
bulk the AMS target material with bromine and/or natural-ratio chlorine solutions, without adding  $^{37}\text{Cl}$ -enriched spike.  
Experiments on seven geologic test samples reveal that the workflow presented here yields comparable or, in the case of the  
380  $^{35}\text{Cl}/^{37}\text{Cl}$  measurements, improved results over the traditional workflow. Most notably, by measuring  $^{35}\text{Cl}/^{37}\text{Cl}$  on a ~1 g aliquot  
rather than a 20 g sample, the new preparation methods use up to 95% less of the isotopically enriched spike solution than  
standard methods (~50-75  $\mu\text{g Cl}$  versus ~750-1000  $\mu\text{g Cl}$ ). With lowered spike solution requirements, researchers can analyze  
many more samples using their remaining laboratory resources. Chlorine extraction laboratories will also be able to maintain  
control over the total chlorine content within and across analytical batches. Finally, in comparison to the standard  $^{36}\text{Cl}$   
385 workflow, our method can identify samples with elevated native Cl concentrations at earlier stage of laboratory work, which  
can help researchers determine which of their rock samples should be prioritized for  $^{36}\text{Cl}$  analyses. Our hope is that these  
procedures will supplement existing laboratory and AMS workflows for cosmogenic Cl and enhance the effectiveness of  $^{36}\text{Cl}$   
dating for a variety of geologic applications.

## 390 Data availability

All data are presented in Tables 1-4 of this technical note.



### Author contribution

AJL and JML carried out the laboratory work. AJH and TSA made the  $^{36}\text{Cl}/\text{Cl}$  and  $^{35}\text{Cl}/^{37}\text{Cl}$  measurements. AJL wrote the first draft of the manuscript, and all authors contributed to experimental design, data analysis, and manuscript review and editing.

### Competing interests

The authors declare that they have no competing interests.

### 400 Acknowledgements

AJL acknowledges funding from Queens College. Prepared in part by LLNL under Contract DE-AC52-07NA27344. This is LLNL-JRNL-861073.

### References

- Anderson, T. S., Hidy, A. J., Boyce, J. W., McCubbin, F. M., Tumey, S., Dudley, J. M., Haney, N. C., Bardoux, G., and Bonifacie, M.: Development towards stable chlorine isotope measurements of astromaterials using the modified Middleton source of an accelerator mass spectrometer, *Int J Mass Spectrom*, 477, 116849, <https://doi.org/10.1016/J.IJMS.2022.116849>, 2022.
- Arnold, M., Merchel, S., Boursès, D. L., Braucher, R., Benedetti, L., Finkel, R. C., Aumaître, G., Gott dang, A., and Klein, M.: The French accelerator mass spectrometry facility ASTER: Improved performance and developments, *Nucl Instrum Methods Phys Res B*, 268, 1954–1959, 2010.
- Barth, A. M., Marcott, S. A., Licciardi, J. M., and Shakun, J. D.: Deglacial Thinning of the Laurentide Ice Sheet in the Adirondack Mountains, New York, USA, Revealed by  $^{36}\text{Cl}$  Exposure Dating, *Paleoceanogr Paleoclimatol*, 34, 946–953, <https://doi.org/10.1029/2018PA003477>, 2019.
- Ben-Asher, M., Haviv, I., Crouvi, O., Roering, J. J., and Matmon, A.: The convexity of carbonate hilltops:  $^{36}\text{Cl}$  constraints on denudation and chemical weathering rates and implications for hillslope curvature, *GSA Bulletin*, 2021.
- Benedetti, L., Finkel, R., Papanastassiou, D., King, G., Armijo, R., Ryerson, F., Farber, D., and Flerit, F.: Post-glacial slip history of the Sparta fault (Greece) determined by  $^{36}\text{Cl}$  cosmogenic dating: Evidence for non-periodic earthquakes, *Geophys Res Lett*, 29, 87–1, <https://doi.org/10.1029/2001GL014510>, 2002.



- Eberlein, G. D., Churkin, M., Carter, C., Berg, H. C., and Ovenshine, A. T.: Geology of the Craig quadrangle, Alaska, US  
420 Geological Survey, 1983.
- Faure, G. and Mensing, T. M.: *Isotopes: Principles and Applications*, Third edition., John Wiley and Sons, Hoboken, New  
Jersey, 2005.
- Finkel, R., Arnold, M., Aumaître, G., Benedetti, L., Bourlès, D., Keddadouche, K., and Merchel, S.: Improved  $^{36}\text{Cl}$   
performance at the ASTER HVE 5 MV accelerator mass spectrometer national facility, *Nucl Instrum Methods Phys Res B*,  
425 294, 121–125, 2013.
- Gosse, J. C. and Phillips, F. M.: Terrestrial in situ cosmogenic nuclides: Theory and application, *Quat Sci Rev*, 20, 1475–1560,  
[https://doi.org/10.1016/S0277-3791\(00\)00171-2](https://doi.org/10.1016/S0277-3791(00)00171-2), 2001.
- Ivy-Ochs, S., Poschinger, A. V., Synal, H.-A., and Maisch, M.: Surface exposure dating of the Flims landslide, Graubünden,  
Switzerland, *Geomorphology*, 103, 104–112, 2009.
- 430 Kozaci, O., Dolan, J., Finkel, R., and Hartleb, R.: Late Holocene slip rate for the North Anatolian fault, Turkey, from  
cosmogenic  $^{36}\text{Cl}$  geochronology: Implications for the constancy of fault loading and strain release rates, *Geology*, 35, 867–  
870, 2007.
- Licciardi, J. M. and Pierce, K. L.: History and dynamics of the Greater Yellowstone Glacial System during the last two  
glaciations, *Quat Sci Rev*, 200, 1–33, 2018.
- 435 Licciardi, J. M., Denoncourt, C. L., and Finkel, R. C.: Cosmogenic  $^{36}\text{Cl}$  production rates from Ca spallation in Iceland, *Earth  
Planet Sci Lett*, 267, 365–377, <https://doi.org/10.1016/J.EPSL.2007.11.036>, 2008.
- Marrero, S. M., Phillips, F. M., Caffee, M. W., and Gosse, J. C.: CRONUS-Earth cosmogenic  $^{36}\text{Cl}$  calibration, *Quat  
Geochronol*, 31, 199–219, 2016.
- Marrero, S. M., Hein, A. S., Naylor, M., Attal, M., Shanks, R., Winter, K., Woodward, J., Dunning, S., Westoby, M., and  
440 Sugden, D.: Controls on subaerial erosion rates in Antarctica, *Earth Planet Sci Lett*, 501, 56–66,  
<https://doi.org/10.1016/J.EPSL.2018.08.018>, 2018.
- Mitchell, S. G., Matmon, A., Bierman, P. R., Enzel, Y., Caffee, M., and Rizzo, D.: Displacement history of a limestone normal  
fault scarp, northern Israel, from cosmogenic  $^{36}\text{Cl}$ , *J Geophys Res Solid Earth*, 106, 4247–4264,  
<https://doi.org/10.1029/2000JB900373>, 2001.
- 445 Pánek, T., Lenart, J., Hradecký, J., Hercman, H., Braucher, R., Šilhán, K., and Škarpich, V.: Coastal cliffs, rock-slope failures  
and Late Quaternary transgressions of the Black Sea along southern Crimea, *Quat Sci Rev*, 181, 76–92, 2018.
- Parmelee, D. E. F., Kyle, P. R., Kurz, M. D., Marrero, S. M., and Phillips, F. M.: A new Holocene eruptive history of Erebus  
volcano, Antarctica using cosmogenic  $^3\text{He}$  and  $^{36}\text{Cl}$  exposure ages, *Quat Geochronol*, 30, 114–131, 2015.
- Phillips, F. M., Zreda, M. G., Gosse, J. C., Klein, J., Evenson, E. B., Hall, R. D., Chadwick, O. A., and Sharma, P.: Cosmogenic  
450  $^{36}\text{Cl}$  and  $^{10}\text{Be}$  ages of Quaternary glacial and fluvial deposits of the Wind River Range, Wyoming, *Geol Soc Am Bull*, 109,  
1453–1463, 1997.



- Price, B. N., Stansell, N. D., Fernández, A., Licciardi, J. M., Lesnek, A. J., Muñoz, A., Sorensen, M. K., Jaque Castillo, E., Shutkin, T., Ciocca, I., and Galilea, I.: Chlorine-36 Surface Exposure Dating of Late Holocene Moraines and Glacial Mass Balance Modeling, Monte Sierra Nevada, South-Central Chilean Andes (38°S), *Front Earth Sci* (Lausanne), 10, 848652, 455 <https://doi.org/10.3389/FEART.2022.848652/BIBTEX>, 2022.
- Riehle, J. R., Brew, D. A., and Lanphere, M. A.: Geologic map of the Mount Edgecumbe volcanic field, Kruzof Island, southeastern Alaska, 1989.
- Robertson, J., Meschis, M., Roberts, G. P., Ganas, A., and Gheorghiu, D. M.: Temporally constant Quaternary uplift rates and their relationship with extensional upper-plate faults in south Crete (Greece), constrained with  $^{36}\text{Cl}$  cosmogenic exposure 460 dating, *Tectonics*, 38, 1189–1222, 2019.
- Schlagenhauf, A., Manighetti, I., Benedetti, L., Gaudemer, Y., Finkel, R., Malavieille, J., and Pou, K.: Earthquake supercycles in Central Italy, inferred from  $^{36}\text{Cl}$  exposure dating, *Earth Planet Sci Lett*, 307, 487–500, <https://doi.org/10.1016/J.EPSL.2011.05.022>, 2011.
- Sharma, P., Kubik, P. W., Fehn, U., Gove, H. E., Nishiizumi, K., and Elmore, D.: Development of  $^{36}\text{Cl}$  standards for AMS, 465 *Nucl Instrum Methods Phys Res B*, 52, 410–415, [https://doi.org/10.1016/0168-583X\(90\)90447-3](https://doi.org/10.1016/0168-583X(90)90447-3), 1990.
- Singer, B. S., Le Mével, H., Licciardi, J. M., Córdova, L., Tikoff, B., Garibaldi, N., Andersen, N. L., Diefenbach, A. K., and Feigl, K. L.: Geomorphic expression of rapid Holocene silicic magma reservoir growth beneath Laguna del Maule, Chile, *Sci Adv*, 4, eaat1513, 2018.
- Small, D., Rinterknecht, V., Austin, W. E. N., Bates, R., Benn, D. I., Scourse, J. D., Bourlès, D. L., Hibbert, F. D., and Team, 470 A.: Implications of  $^{36}\text{Cl}$  exposure ages from Skye, northwest Scotland for the timing of ice stream deglaciation and deglacial ice dynamics, *Quat Sci Rev*, 150, 130–145, 2016.
- Stone, J. O., Allan, G. L., Fifield, L. K., and Cresswell, R. G.: Cosmogenic chlorine-36 from calcium spallation, *Geochim Cosmochim Acta*, 60, 679–692, 1996.
- Walcott, C. K., Briner, J. P., Baichtal, J. F., Lesnek, A. J., and Licciardi, J. M.: Cosmogenic ages indicate no MIS 2 refugia in 475 the Alexander Archipelago, Alaska, *Geochronology*, 4, 191–211, <https://doi.org/10.5194/GCHRON-4-191-2022>, 2022.
- Wilcken, K. M., Freeman, S., Schnabel, C., Binnie, S. A., Xu, S., and Phillips, R. J.:  $^{36}\text{Cl}$  accelerator mass spectrometry with a bespoke instrument, *Nucl Instrum Methods Phys Res B*, 294, 107–114, 2013.
- Zerathe, S., Lebourg, T., Braucher, R., and Bourlès, D.: Mid-Holocene cluster of large-scale landslides revealed in the Southwestern Alps by  $^{36}\text{Cl}$  dating. Insight on an Alpine-scale landslide activity, *Quat Sci Rev*, 90, 106–127, 2014.